Experimental and Numerical Modal Analysis of Complete and Partial Bonding States of Single-Lap Adhesive Joints

Setareh Garazhian, Milad Shabani Yousefabad , Morteza Homayoun Sadeghi , Mir Mohammad Ettefagh*, Hasan Biglari, Karim Shelesh-Nezhad

Department of Mechanical Engineering, University of Tabriz, Tabriz, Iran

Abstract

This study evaluates the sensitivity of modal parameters to incomplete adhesion in single-lap adhesive joints by comparing the vibrational behavior of fully bonded joints and joints with a macroscopic partial bond (≈50% loss of bonded area in the overlap). Beyond prior studies on crack-like or delamination-type defects, often using intrusive or destructive inspections, the present work targets a practically relevant macroscopic manufacturing flaw within a fully non-destructive modal testing framework. An integrated experimental–numerical approach is employed: aluminum 7075-T6 beams bonded with epoxy 828 are tested using impact-hammer excitation and laser Doppler vibrometer, and responses are processed in MATLAB and MEscope to extract natural frequencies and damping ratios. A three-dimensional finite element model in Abaqus/CAE is refined via limited experimental calibration. Results show 3–15% reductions in the first eight bending natural frequencies of defective joints relative to intact ones, with stronger effects in higher modes due to dominant stiffness loss over minor mass reduction. The damping ratio increases about sevenfold (0.0032 to 0.0236) in the defective specimen, attributed to frictional dissipation at the unbonded interface and contact nonlinearities supported by mode-shape analysis. These quantified shifts in frequency and damping establish modal parameters as reliable, non-destructive indicators of incomplete adhesion in single-lap joints and provide a basis for vibration-based structural health monitoring and defect detection in adhesively bonded components in aerospace, automotive, and multi-material structures.

KEYWORDS

Adhesive Joints, Modal Analysis, Finite Element Method (FEM), Adhesive Defects, Non-destructive SHM

1. Introduction

The choice of joining techniques —whether mechanical fastening, welding, adhesive bonding, or other methods—significantly influences the strength, performance, and service life of structures [1-3]. In recent years, adhesive bonding has garnered considerable attention across a wide range of industries—including aerospace, automotive, electronics, and construction—due to its inherent advantages, such as the ability to bond dissimilar materials more easily, uniform stress distribution across the bonding interface, low density, and the resultant reduction in overall structural weight, which contributes to enhanced durability [1, 2, 4-6].

Despite these advantages, adhesive joints also introduce specific challenges compared with more conventional mechanical fastening or welding [1, 2, 4]. One of the primary concerns is the quality of the bond itself. The presence of air bubbles (voids), porosity, adhesive discontinuities, surface defects, cracks, misalignment, local adhesive separation, wrinkling, delamination, or other imperfections within the adhesive

* Corresponding author E-mail address: ettefagh@tabrizu.ac.ir

layer can locally reduce or even completely interrupt load transfer across parts of the overlap [1, 6, 7]. Such bond defects may effectively create weak or unbonded regions that markedly diminish the strength and stiffness of the joint and can, in turn, lead to undesirable vibrations and even premature failure of the host structure [1, 4, 8-11].

Given the potential presence of such imperfections in the adhesive layer, a reliable characterization of the behavior of adhesive joints is essential [1, 2, 4]. The mechanical response of the bonded region—governed by properties such as stiffness, strength, and resistance to damage and fatigue—directly controls how loads are transferred between adherends and how the joint contributes to the overall performance and safety of the structure under service conditions [1, 2, 12, 13].

Among the different ways to characterize bonded joints—such as static testing, fracture and fatigue experiments, and local inspection techniques—the analysis of vibrational and modal properties offers an attractive alternative [2]. Modal parameters, including natural frequencies, mode shapes and damping ratio, are highly sensitive to changes in stiffness and mass distribution in the bonded region and can be obtained non-destructively on the assembled structure [2, 9]. As a result, vibration-based approaches have become an important tool for assessing the condition of adhesively bonded joints and for supporting structural design, optimization, and health monitoring [2, 12, 13].

Recent advances in adhesively bonded joints (ABJs) indicate a clear transition from strength-only design toward an integrated paradigm that jointly considers joint architecture, manufacturing quality, and long-term in-service performance. Wei et al. [1] provide a comprehensive synthesis spanning joint geometries, adhesive formulations and toughening strategies, surface preparation, curing, experimental characterization, and multiscale modeling for composite and hybrid structures. Their review underscores how tailored configurations (e.g., stepped-lap and scarf joints), improved interfacial treatments, and modified adhesives are increasingly leveraged to reconcile stiffness, strength, durability, and weight efficiency. Nonetheless, several critical bottlenecks persist. Predicting damage initiation and evolution under coupled dynamic and hygrothermal exposure remains challenging, given the strong sensitivity of adhesive and interface behavior to temperature–moisture histories. In parallel, thin bondlines amplify the impact of manufacturing variability and defects, motivating more reliable quality assurance and defect detectability. Finally, robust, experimentally validated models suitable for optimization and digital-twin integration are still needed.

Ramalho et al. [2], in a comprehensive review article, examined the dynamic behavior of adhesive joints and categorized related numerical investigations into three primary domains: fatigue, variable strain-rate and impact loading, and modal analysis. Numerical studies in these areas can be carried out using various approaches such as continuum mechanics, damage mechanics, fracture mechanics, and cohesive zone modeling. By presenting both numerical and theoretical investigations and systematically relating them to the available experimental findings reported in the literature, the authors underscored the practical significance of considering the dynamic behavior of adhesive joints, particularly highlighting the role of numerical analysis in the design and optimization of such joints across multiple industries, including automotive engineering and wind turbine systems. The limitations of their study were mainly associated with the need for further research to enhance the applicability of findings—especially in the field of modal analysis—as well as the necessity for additional experimental data to validate and calibrate numerical models.

Marchione [4] investigated the influence of a notch, introduced in one of the adherends (placed in the mid-layer) while the adhesive layer was assumed to remain intact, on the vibrational and dynamic characteristics of adhesively bonded structures with various material combinations in a double-lap joint configuration. The study focused on double-lap specimens with different adherend pairings, including aluminum–glass, GFRP–glass, and steel (S235JR)–glass. Both pristine and defective samples—featuring notches of three different depths (1, 2, and 3 mm)—were analyzed for each material combination. Thus, the two key variables examined in this study were the presence and depth of the notch, and the type of adherend material. The analysis, conducted via finite element modeling using ANSYS, focused on evaluating the

natural frequencies and performing modal analysis. The results indicated that the natural frequencies are significantly influenced by the Young's modulus and the density ratio, both of which vary depending on the material used. Moreover, the presence of a notch notably affected the vibrational behavior at higher frequencies. However, the reduction in mass caused by the notch did not alter the general pattern of mode shapes. Marchione concluded that the introduction of a crack or notch does not exert a substantial effect on the overall dynamic response of the structure.

Basri et al. [5] focused their research on model updating by defining and comparing various finite elements in order to identify the most accurate element type that yields the highest correlation between numerical simulations and experimental results. The structures under investigation were composite bonded assemblies with a panel-to-hat joint configuration, incorporating dual epoxy-based carbon fiber-reinforced flanges. The finite element modeling was conducted using MSC Nastran SOL 200 (2018 edition), with mesh generation performed in HyperMesh (Altair Engineering, MI, US). Experimentally, the structures were evaluated through impact hammer testing under free–free boundary conditions to obtain the vibrational response. Basri emphasized the importance of accounting for multiple influential parameters when assessing element accuracy, including Young's modulus, structural geometry, the thickness of the composite adhesive region, the sensitivity of the shear modulus to torsional frequency response, and the effects of adhesive thickness definition and mesh configuration in the finite element model. Unlike previous studies, Basri highlighted the type of finite element as a significant factor in modal analysis and the identification of dynamic and vibrational characteristics.

Das and Yilmaz [8] conducted both experimental and numerical analyses of the free vibration behavior of curved composite beams containing open transverse cracks. The primary objective was to investigate the effects of crack location and depth on the natural frequencies and mode shapes under various boundary conditions, namely fixed–fixed and fixed–free. Numerical simulations were performed using ANSYS, while the curved composite beams were fabricated via hand lay-up molding. Experimental vibration tests were conducted using an impact hammer and accelerometer sensors, followed by data acquisition through a laser measurement system and subsequent analysis using dedicated software. The study revealed that the influence of crack depth and position on natural frequencies depends significantly on the boundary conditions and the specific dynamic behavior of the beam. Cracks were identified as critical points affecting vibrational response, with an overall trend of decreasing natural frequencies as crack depth increased. However, the authors noted that cracks can sometimes act as local supports, enhancing localized stiffness and, consequently, causing increases in natural frequencies for certain vibration modes.

Agarwalla and Parhi [9] investigated the modal parameters of a cracked cantilever beam through a combination of theoretical analysis, numerical modeling, and experimental testing. In their theoretical approach, the crack was modeled as a massless rotational spring. Numerical simulations and vibrational analysis were carried out using ANSYS, while experimental validation involved vibration tests using accelerometers and vibration analyzers. By comparing the results with those of an intact cantilever beam, the study revealed a reduction in natural frequencies and notable alterations in the mode shapes due to the presence of the crack.

Aslam et al. [10] investigated the dynamic response of smart piezoelectric structures by examining the effects of adhesive debonding in cantilever beams. Utilizing three-dimensional finite element modeling and simulations performed in Abaqus/CAE, the study demonstrated that partial adhesive debonding has a significant impact on resonant frequencies, displacement amplitudes, and wave signal characteristics. The research highlighted the critical role of the adhesive layer in transmitting forces and stresses between the piezoelectric layer—composed of lead zirconate titanate (PZT)—and the host structure. The authors emphasized the necessity of incorporating the adhesive interface in numerical models to ensure accurate prediction of structural behavior.

Patil et al. [11] conducted a numerical modal analysis to gain deeper insight into the dynamic behavior of defect-free single-lap adhesive joints (SLJs) in adhesively bonded metallic beams composed of identical

adherends. The study considered metallic adherends made of aluminum, copper, and manganese bonded with an epoxy-based adhesive, keeping the joint geometry fixed. The samples, defined by specific geometries and material properties, were modeled using the finite element software ANSYS, and the corresponding natural frequencies and mode shapes were extracted and reported. The authors emphasized the role of natural frequencies and mode shapes in predicting the structural response under dynamic loading conditions. Their findings revealed that the natural frequencies exhibit a relationship with both the elastic modulus (Young's modulus) and the material density of the adherends. However, the scope of the study was limited to only three metallic adherend materials, a single type of adhesive, and a single joint configuration. Moreover, the absence of experimental validation restricts the generalizability of the conclusions, indicating the need for further studies to achieve more robust and reliable results.

Lee [14] conducted a study on the free vibration analysis of laminated composite beams. Utilizing a layer-wise modeling approach in conjunction with the finite element method, the research examined the influence of various delamination parameters—such as size, location, and number of delaminations, as well as fiber orientation—on the natural frequencies and mode shapes. The results indicated that larger delaminations, especially those located at the mid-span of the beam, have a more pronounced effect on reducing the natural frequencies. Furthermore, higher fiber orientation angles ($\theta > 45°$) were found to exacerbate the impact of delaminations. The extended layer-wise model demonstrated high accuracy in predicting the dynamic behavior of the structure and was capable of capturing localized modes associated with the delaminated regions. This study provides valuable insights for the design and optimization of laminated composite structures. However, this contribution is limited to idealized one-dimensional beams with through-the-width delaminations and linear kinematics, and the study is purely numerical, without experimental validation of the predicted natural frequencies and mode shapes.

Wang et al. [15] conducted a notable study on the dynamic behavior of adhesively bonded beams using a layered finite element method. Each adhesive and adherend layer was modeled independently to assess the effects of geometric parameters (e.g., overlap length, adhesive thickness), mechanical properties of different adherend materials (e.g., aluminum, nickel), and joint configuration (stepped or unstepped). The study evaluated modal frequencies, damping ratios, and vibration amplitudes through MATLAB coding and Lanczos/Arnoldi solvers, with validation against experimental data. Results highlighted that increasing overlap length raised natural frequencies, while thicker adhesive layers reduced them but improved damping. Despite its effectiveness, the study was limited by simplified geometry, material selection, and lack of environmental considerations.

Chinka et al. [16] employed a frequency mode shape-based damage detection (FMBDD) approach to identify the location and depth of cracks in cantilever beams using modal parameters such as natural frequencies and mode shape curvature. Both theoretical and experimental investigations demonstrated that variations in higher-order natural frequencies and localized changes in the curvature of mode shapes near the crack zone enable accurate crack identification. This method not only reduces computational effort but also offers high accuracy in damage detection within beam-like structures, making it a valuable tool for structural health monitoring (SHM) applications.

In another study, Sahu et al. [17] investigated the influence of transverse cracks on the natural frequencies of isotropic beams under free vibration using finite element analysis in Abaqus/CAE. The results revealed that both the location and depth of the crack—particularly when the crack is situated near the support or at the mid-span—have a significant impact on the reduction of natural frequencies. The study also emphasized that the boundary conditions of the beam play a critical role in its dynamic behavior.

Behera et al. [18] investigated the effect of pre-embedded defects—adhesive disbonds and surface delaminations—on the structural integrity of single-lap adhesive joints made of curved composite panels bonded with an epoxy adhesive. Three-dimensional finite element models incorporating the Virtual Crack Closure Technique (VCCT) were used to compute the strain energy release rate (SERR) for different fracture modes (opening, longitudinal shear, and transverse shear) at high stress-concentration regions. The results

showed that longitudinal shear is the dominant failure mode in these joints, and that higher SERR values lead to faster damage growth, with delaminations near the overlap edges propagating more rapidly and adhesive defects close to the outer surface having the most detrimental impact on joint integrity. The study highlights how the type, size, and location of manufacturing defects critically influence failure behavior in safety-critical structures such as aircraft fuselages, wind turbine blades, and marine components, though its scope is limited to specific defect configurations, neglects environmental effects, and relies on a relatively complex numerical framework.

Pazand and Nobari [19] investigated the effect of damage on the dynamic mechanical properties of viscoelastic adhesives, with particular emphasis on variations in Young's modulus and shear modulus within both linear and nonlinear response regimes. Healthy and damaged single-lap joints were prepared, where Teflon inserts were used to simulate damage. Linear and nonlinear frequency response functions were measured and compared with numerical results obtained from finite element modeling using ANSYS. The findings demonstrated that the mechanical moduli of the adhesive were highly sensitive to both excitation frequency and damage location. Even minor defects were shown to significantly affect the dynamic behavior of the bonded structure.

In a recent study, Ordonneau et al. [20] developed a mixed analytical–numerical (matrix exponential, ME) formulation for the modal analysis of single-lap adhesive joints and validated it against a spring-based finite element (FE) model (beam elements plus shear/peel springs for the adhesive) implemented in PATRAN/NASTRAN under both balanced and unbalanced configurations and free–free and clamped–free boundary conditions. The comparison showed excellent agreement, with discrepancies in natural frequencies typically below 0.1% for 1D bars and 0.5% for 1D beams, demonstrating the high accuracy and efficiency of the ME approach with far fewer degrees of freedom. The authors then modeled the adhesive as a functionally graded layer with a parabolic variation of shear and tensile stiffness along the overlap, and reported that even non-uniform, graded adhesive properties modify the natural frequencies only marginally (≈0.5–2% increase), indicating that such grading primarily reduces local stress concentrations rather than fundamentally altering global vibrational behavior. However, the work is limited to idealized one-dimensional joint representations without experimental validation or explicit consideration of discrete macroscopic defects in the bonded region.

Nwankwo et al. [21] performed combined experimental, analytical, and finite element studies on interfacial stresses in single-lap adhesive joints subjected to transverse impact loading. They derived a Hamilton-based analytical model for peel and shear stresses in a linearly elastic adhesive, reduced the governing equations via the Galerkin method, and solved them using the Newmark-β scheme, then validated against a refined C3D8R Abaqus model. Their results showed that maximum peel and shear stresses occur at the lower edge of the overlap, with peel stresses dominant and clear indications of debonding initiation at the joint ends. Although the analytical model reproduced peak interfacial stresses well, it could not capture the full time history or crack growth, limiting its use for fracture-mechanics-based failure prediction.

Melro and Liu [22] introduced a model-updating strategy for single-lap adhesive joints in which the effective Young's modulus of the overlap region is identified using a transfer matrix method (TMM). By adjusting this effective modulus to match theoretical and target natural frequencies, and benchmarking against COMSOL simulations and experimental tensile characterization of the adhesive, they demonstrated superior agreement compared with conventional collective updating schemes. Their approach highlights the potential of single-parameter TMM-based updating to represent the dynamic stiffness of the bonded region efficiently. However, the lack of direct modal testing data restricts the robustness of the dynamic validation.

García-Barruetabeña and Cortés [23] conducted a finite element investigation of the vibration response of adhesively bonded beams with viscoelastic adhesive layers, calibrated against previous experimental measurements. Using isoparametric elements and the Boltzmann superposition principle, they studied the effects of overlap length, adhesive thickness, storage modulus **E'**, and loss factor η on resonant frequencies, amplitudes, and modal loss factors. They found that increasing overlap length raises resonant frequencies,

while greater adhesive thickness lowers frequencies but enhances damping, and higher loss factors significantly reduce resonance amplitudes and increase modal attenuation. Their work underscores the key role of joint geometry and adhesive viscoelasticity in vibration and noise control of bonded structures.

Gunes et al. [24] analyzed the free vibration of adhesively bonded single-lap joints with functionally graded adherend plates composed of Al_2O_3/Ni, modeled via power-law material gradation. Using ANSYS with SOLID95 elements for the adhesive and SHELL99 layered elements for the plates, complemented by neural-network-based frequency prediction, they examined the influence of width, thickness, overlap length, and gradation index on the first several natural frequencies and mode shapes. Their results showed that wider plates substantially reduce, and thicker plates markedly increase, natural frequencies, while overlap length has only a minor effect; increasing the ceramic fraction consistently raises frequencies through higher stiffness. Although insightful for FGM-based joint design, the specialized material system and simplifying assumptions limit the general applicability of the conclusions to conventional metallic lap joints.

Electromechanical impedance spectroscopy (EMIS) has recently been explored as a localized SHM tool for adhesively bonded joints, but existing studies on void detection remain limited and strongly adhesive-dependent. Tenreiro et al. [25] investigated artificial cavity damage in single-lap joints bonded with a modified epoxy and a pressure-sensitive adhesive (PSA), combining experiments and ABAQUS simulations. Their results showed that voids in the epoxy joints produced clear changes in the impedance spectra, with frequency shifts and amplitude variations that enabled reliable damage detection, whereas similar voids in PSA joints led to negligible spectral changes, indicating poor sensitivity for that adhesive system. The authors also highlighted practical limitations, including unintended secondary damage around drilled cavities, possible property variations in manually mixed adhesives, strong influence of boundary conditions on the impedance response, and the challenges of accurately modeling multi-dimensional mechanical impedance.

Therefore, the investigation of the mechanical and vibrational characteristics of adhesive joints has become increasingly essential. In many previous studies, defects were predominantly considered in the form of cracks, notches, or delaminations. Unlike these 1D or 2D defects, macro voids and half-overlap area disbonding represent very significant and hazardous manufacturing defects that compromise substantial bonded area. In fact, the vibrational behavior of adhesive joints in the presence of such larger-scale defects—with substantial volume area—and their impact on modal parameters has been relatively underexplored. In the present study, through a combination of experimental and numerical modal analysis, we assess the feasibility of non-destructive detection of these defects on the dynamic and vibrational characteristics of single-lap adhesive joints from the perspective of system integrity assessment.

2. Modal Analysis Of Adhesive Joints

Modal analysis is one of the most widely used non-destructive techniques for identifying the vibrational characteristics of a system, aiming to determine key parameters such as natural frequencies, mode shapes, and damping ratios, which in turn provide insight into the physical properties of the structure—namely mass, stiffness, and damping [6, 11, 13]. In experimental modal analysis, the structure is excited by external means such as impact, vibration, or displacement, and the resulting dynamic response is recorded using measurement devices such as accelerometers or laser vibrometers[8]. These response signals are then analyzed to extract the modal parameters[13, 26]. In numerical modal analysis, a mathematical model of the system is constructed, and numerical methods are used to compute the modal properties. Within the technical literature, it is common practice to perform numerical modal analysis through finite element modeling (FEM) of the structure and its boundary conditions using specialized software tools [13, 27].

2.1. Specimens Fabrication

The selected adhesive joint configuration is of the single-lap type, constructed using 7075-T6 aluminum alloy and bonded with Epoxy Resin 828 and TETA hardener in a mixing ratio of 100:13 by weight. Aluminum sheets made from 7075-T6 alloy, with thicknesses of 1.8 mm, were sourced from Amag—an Austrian company renowned for its precision manufacturing of high-strength aluminum alloys using advanced technologies and emphasizing superior strength-to-weight ratios. The chemical composition of the 7075-T6 alloy includes 87–91% aluminum, 5.6–6.1% zinc, 2.1–2.5% magnesium, 1.2–1.6% copper, and less than 0.5% of other metals such as iron, silicon, chromium, manganese, and titanium. According to ASTM E756 [12], which outlines the procedures for dynamic mechanical testing of materials, the components may be tested in customized dimensions appropriate for vibrational studies [12]. It is worth noting that the final mechanical properties of the adhesive—such as hardness, flexibility, and Young's modulus—depend on the epoxy-to-hardener mixing ratio [28]. A summary of the key material properties used in this research, essential for modeling and interpretation, is provided in Table 1.

Table 1. Selected Mechanical Properties of the Materials Employed

Material	Young's Modulus (GPa)	Poisson's Ratio	Density (Kg/m^3)
AL7075-T6	71.7	0.32	2810
EPOXY 828+ HARDNER TETA	2.5-3.2	0.35	1150

Four rectangular specimens with dimensions of 124 × 25.4 × 1.8 mm were machined from 7075-T6 aluminum sheets with the aforementioned properties using a wire-EDM (Electrical Discharge Machining) process. To ensure proper curing of the adhesive and guarantee precise alignment and adhesive thickness control, an appropriate fixture was utilized for specimen holding during bonding.

The fixture was prepared through thorough cleaning and sanding to remove any contaminants or misalignments. It consisted of the following components: two deep steel beams—one fixed and one adjustable/movable; a supporting bottom plate; multiple bolts and nuts for securely fastening the steel beams to maintain alignment; and an upper bolt and nut assembly for applying the bonding pressure and adjusting the adhesive layer thickness. Fig. 1 shows the fixture along with a specimen being positioned inside it.

Fig. 1. Adhesive curing fixture designed for specimen placement and alignment control.

Preparation of Specimens for Adhesive Application:

The preparation of the machined specimens for adhesive bonding involved the following steps:

- Washing the specimens with soap and water, followed by drying with a lint-free cloth.

- Sanding the adhesive area, which is 25 mm from the edge of each specimen, using 120-grit sandpaper in a strictly parallel horizontal stroke pattern. If surface contamination was present on the specimens, the entire surface was sanded in a direction opposite to that of the adhesive area sanding. All specimens were sanded uniformly following this procedure.
- Cleaning the specimens with acetone.
- Rinsing the specimens with distilled water and allowing them to air dry completely.
- Marking the adhesive application area and the back side of the adhesive region (to indicate the position of the clamping screws) using a permanent marker.
- Applying a release agent (wax) to areas where adhesive bonding was not desired; for the defective specimen, a separating foil was inserted over half of the overlap area to simulate a defect [1].

And also the adhesive was prepared and applied as follows:

- Initially, 5 grams of epoxy resin and 0.65 grams of hardener were precisely weighed using a scale and poured into a mixing container.
- The mixture was stirred gently in a clockwise direction for 3 minutes, taking care to avoid the formation of air bubbles.
- Adhesive was applied to the bonding surfaces of both specimens, noting that only 1 minute was allowed for this process.
- Finally, the two adhesive-coated ends were overlapped and the specimen was placed inside the fixture[28].

After 24 hours, the adhesive fully cured, allowing the specimens to be removed from the fixture [7]. Seven days post-bonding, the mechanical properties of the specimens stabilized, permitting subsequent testing [1, 28].Thus, two specimens were prepared: one intact specimen (complete and defect-free bond) and one defective specimen (partial bond) containing a rectangular void defect occupying half of the overlap area.

2.2. Experimental Modal Analysis Testing

Performing experimental modal analysis on the fabricated specimens requires the utilization of specific laboratory equipment, including an impact hammer, laser vibrometer, and an analog-to-digital signal converter. The impact hammer used was a B&K Type 8200 manufactured by Brüel & Kjær (B&K), equipped with a force sensor that enables the measurement and recording of the impact force. A Doppler Laser Vibrometer (LDV) Type VH300 was employed as a non-contact instrument to measure vibrations. This device uses the Doppler effect technique to measure vibration velocity and displacement. Signals obtained from various sensors (such as impact force or vibration response) are transmitted to an analog-to-digital converter, which accurately samples the analog signals at a high rate and converts them into digital data. This data is then transferred via communication ports to analysis software. The converter, a Type 22827 also manufactured by B&K, plays a crucial role in ensuring data quality, noise reduction, and enabling precise frequency-domain analysis of the structural response. The PULSE software, a comprehensive modal and vibration analysis platform developed by Brüel & Kjær, receives the digital signals from the converter and, utilizing advanced signal processing tools including the Fast Fourier Transform (FFT), facilitates the extraction of natural frequencies, mode shapes, and damping parameters. Prior to test setup, a total length of 195 mm of each structure was trimmed from the free end of each specimen to create a fixed boundary condition at the known end. Measurement points for signal acquisition were marked at 55 mm intervals along the specimen length using dots. Excitation was applied both by impact hammering and by inducing free vibration through displacement and release of the free end. The vibration velocity signals on the specimen surface were acquired by the laser Doppler vibrometer at the

predetermined points. To enhance laser light reflection and measurement accuracy, these points were marked with dark paint. It should be noted that before the modal tests, the accelerometer, the laser Doppler vibrometer/optical velocity sensor, and the force transducer of the impact hammer were calibrated using a Brüel & Kjær Calibration Exciter Type 4294 according to the manufacturer's procedure, and the corresponding sensitivity factors in the acquisition software were adjusted to match the reference signal. Fig. 2 shows the test's equipment and specimen separately; and Fig. 3 shows the arrangement of the equipment and specimen during the experimental modal analysis testing.

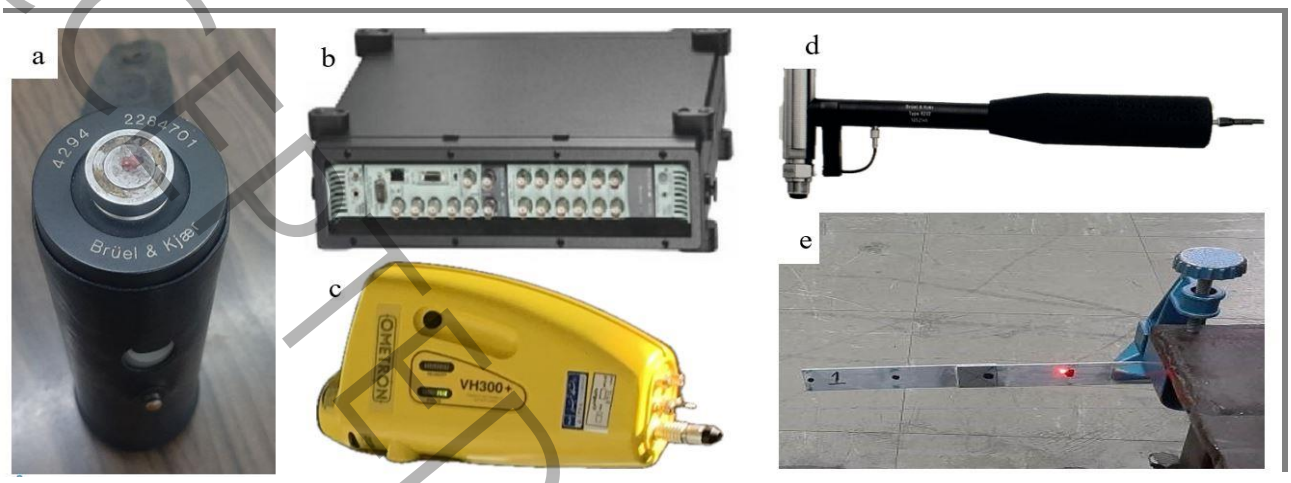

Fig. 2. Equipment and specimen of the experimental modal analysis test: a) Brüel & Kjær Calibration Exciter Type 4294; b) Analog to digital convertor B&K Type 22827; c) Doppler Laser Vibrometer (LDV) Type VH300; d) Impact hammer B&K Type 8200; e) Specimen clamped at the support point.

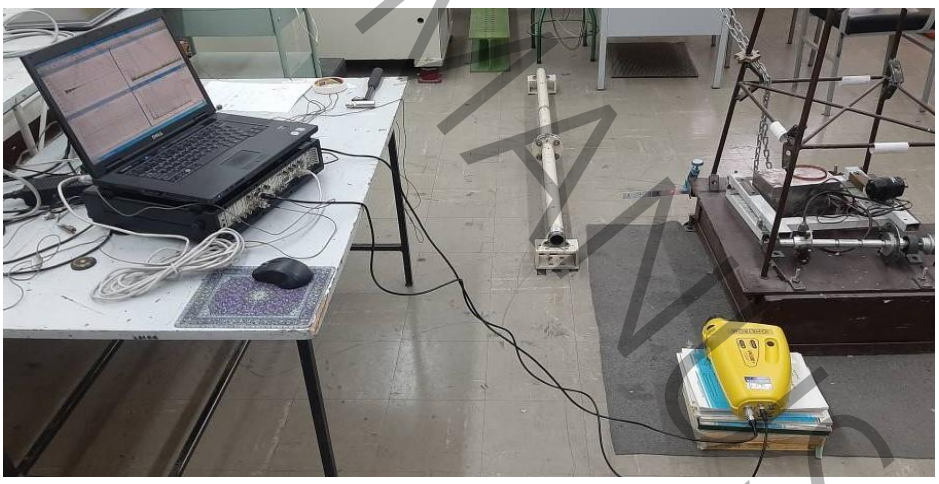

Fig. 3. The arrangement of the equipment and specimen during the experimental modal analysis testing.

Ultimately, the raw data—essentially the impact response signals, which naturally include some level of noise—are recorded at each measurement point on every specimen [26]. Through proper signal analysis, one can evaluate the test conditions and validate the accuracy of the experimental procedure. To this end, various plots such as coherence functions, impact force signals, and vibration response signals are used to assess the system's dynamic behavior and ensure data quality and testing integrity [29]. For further validation and data interpretation, some of the recorded signals are converted into appropriate text-based file formats and imported into MATLAB using custom-written scripts. In MATLAB, these signals are processed and analyzed through plots such as the Frequency Response Function (FRF) and Fast Fourier Transform (FFT) to extract the system's natural frequencies. Additionally, the processed outputs are imported into dedicated modal analysis software such as MEscope to further extract modal parameters. For data processing in

MEscope, all measurement point data—obtained from both impact excitation and free vibration tests—are imported into the software in a clean, noise-filtered format. Peak frequencies are identified by examining signal spectra, and the natural frequency values are read by locking the software's frequency cursor at the prominent peaks. Furthermore, mode shapes and their animated visualizations can be generated and examined within MEscope for better insight into the structural dynamic behavior [26, 29, 30].

2.3. Numerical Modal Analysis (A Finite Element Simulation)

According to the schematics provided in Fig. 4, a three-dimensional finite element model of the single-lap adhesive joint was developed in Abaqus/CAE 2020 using the SI unit system, with the aim of extracting the natural frequencies and mode shapes. The adherend–adhesive interfaces were modeled by surface-based tie constraints, enforcing perfect bonding without separation or sliding. The defective configuration was represented by a rectangular void in the adhesive that removes approximately 50% of the overlap area so that no load transfer occurs in this debonded region. It should be noted that no nonlinear surface-to-surface contact with possible opening or closure was defined; thus, contact loss cannot occur during the modal analysis and the interface conditions remain linear. To replicate the experimental setup, one end of the joint was fully clamped over the same grip length as in the test fixture, and the opposite end was left free, reproducing the cantilever boundary condition used in the laboratory measurements. The model utilized 168 elements of type C3D8R (a three-dimensional linear elastic brick element with eight nodes and reduced integration) for both the aluminum adherends and the epoxy adhesive layer, with a refined mesh in the overlap region. These elements are hexahedral, with each node possessing three translational degrees of

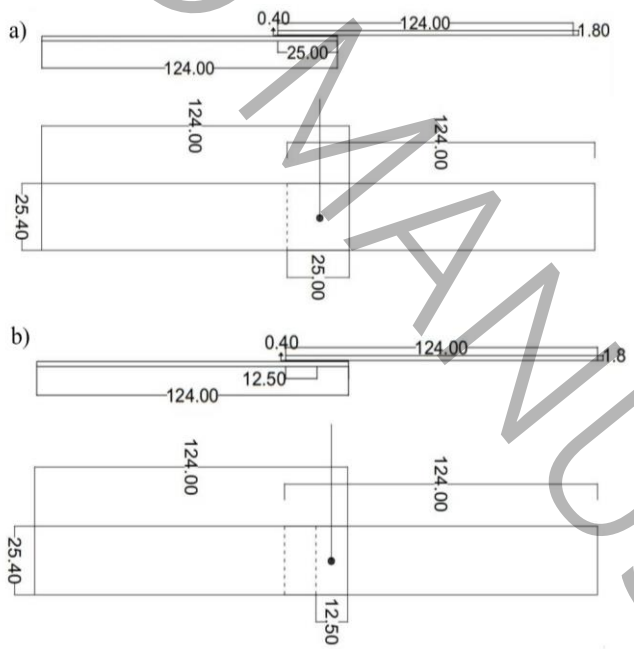

Fig. 4. Technical drawings of : a) The intact specimen, b) The defective specimen (units are in millimeter).

freedom and linear shape functions. The total number of nodes in the model was 420. The mesh size was set to 0.0062 meters, a value recommended by the software as optimal, based on the geometry and analysis requirements. The meshed sample and the modeling of the adhesive region in the single-lap joint configuration are illustrated in Fig. 5. Subsequently, a modal analysis step was carried out using the eigenvalue solver Lanczos in Abaqus/CAE to compute the natural frequencies and corresponding mode shapes of the structure.

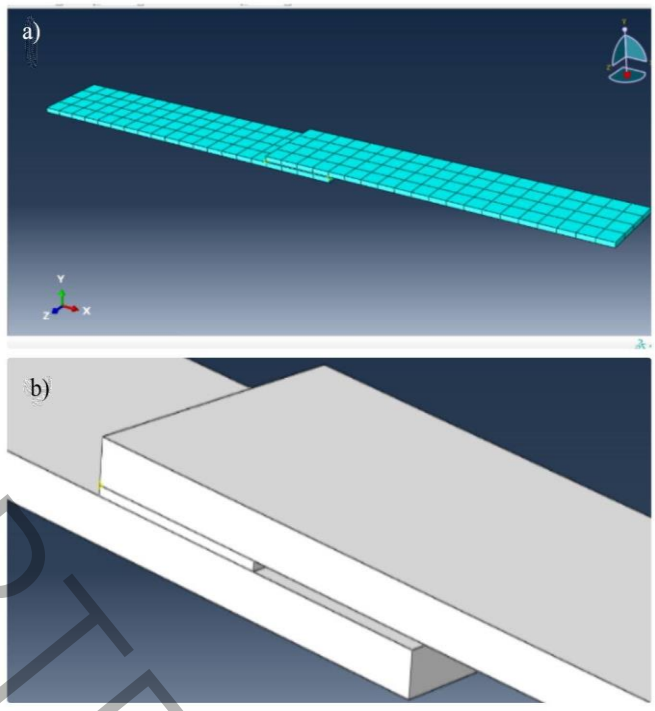

Fig. 5. a) The meshed sample, b) modeling of the overlap region in the defective specimen in fem software.

A mesh sensitivity study was performed for the intact joint by varying the global element size between 0.02 m and 0.002 m and monitoring the first bending natural frequency. As summarized in Table ٢, the difference between the two finest meshes is negligible, and the mesh with an element size of 0.0062 m, which is also the element size suggested by Abaqus/CAE, was therefore adopted as a good compromise between accuracy and computational cost.

Table ٢. Mesh sensitivity analysis for the first bending natural frequency of the intact joint.

Element size (m)	F1 (Hz)	Error vs. finest mesh ε (%)
0.02	22.79	١٧,٥
0.01	17.56	٣٦,٤
0.085	29.810	٧,٨٩
0.062	27.63	٠,٠
0.055	26.283	٤,٩
0.050	26.283	٤,٩
0.003	29.207	٥,٧
0.002	29.207	٥,٧

In experimental modal testing of adhesively bonded joints, some level of uncertainty is unavoidable due to small variations in boundary conditions, clamping stiffness, and signal sensitivity, as well as scatter in the adhesive properties arising from hand lay-up, mixing ratio of epoxy and hardener, and cure conditions. In addition, several studies have reported that the dynamic (frequency-dependent) modulus of epoxy systems can exceed their quasi-static modulus by roughly 10–20% in the glassy region, depending on test method and loading rate [2, 20, 22, 25, 28]. In the present work, these sources of uncertainty are accounted for by a limited calibration of the adhesive material properties, in which the nominal elastic modulus and, to a lesser extent, the density of the adhesive were adjusted slightly within experimentally reported ranges for similar epoxy–hardener systems so that the finite-element model reproduces the measured low-order natural

frequencies with acceptable accuracy. The adherend properties and joint geometry are kept at their nominal values, and the same calibrated adhesive properties are used consistently for both the intact and defective configurations, ensuring that the model remains predictive. In the finite element model, the adhesive layer was therefore characterized by an effective dynamic Young's modulus, $E_{eff,Dyn}$, explored parametrically in the range 5–7 GPa, with $E_{eff,Dyn}$=7 GPa ultimately adopted as a calibrated value that accounts for experimental and modelling uncertainties and yields the best overall agreement with the measured modal data, while being interpreted as an effective stiffness parameter rather than a bulk static material property [22].

3. Results and Discussion

This section evaluates the dynamic and vibrational behavior of adhesive joints under two conditions: a fully bonded (intact) joint and a partially bonded (defective) joint, based on both experimental and numerical findings. Accordingly, several modal parameters are examined to assess the feasibility of damage detection. Furthermore, in order to ensure the accuracy and reliability of the obtained results, the experimental setup and test conditions were thoroughly evaluated for consistency and repeatability.

3.1. Evaluation of Experimental Conditions Using Input and Output Data

In this section, the experimental conditions are evaluated by analyzing the validity of input and output vibrational signals. Utilizing coherence function plots and impact response signals, the accuracy of the data, noise level, and consistency of impact conditions across different specimens were assessed. Fig.s 6 to 10 shows plots extracted from the experimental data, processed using customized MATLAB code. Fig. 6 presents a representative coherence diagram (as the remaining plots exhibited similar patterns, they are not included here for brevity). A coherence value close to 1 indicates a strong correlation between the input and output signals, confirming the high quality of the experimental data. A drop in coherence at specific frequencies may result from measurement noise or experimental inaccuracies [13, 29].

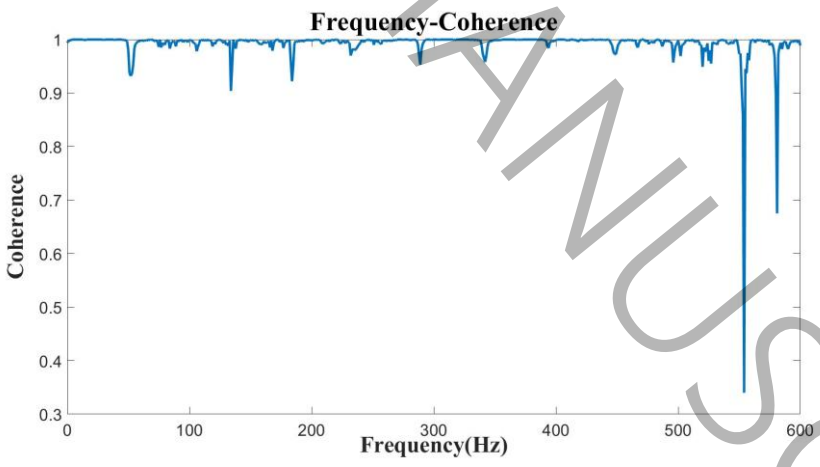

Fig. 6. The coherence diagram extracted by coding in Matlab.

Fig. 7 illustrates a representative impact force signal exerted by the hammer. For each specimen, 12 impacts were applied. The close similarity of these signals indicates a consistent impact force across all tests, confirming the uniformity of experimental execution (Other impact plots are omitted here for brevity). Fig.s 8 shows an example of the impact response signal recorded for respectively the intact adhesive joint and the defective one. The decay behavior of the response is a key parameter in vibration testing. For instance, a rapid decay indicates a high damping ratio in the system [2, 13, 29, 31]. Using the impact response signal and applying the logarithmic decrement method, the damping ratio was calculated [13, 26, 31]. The results revealed that the damping ratio for the intact specimen was 0.0032, while for the defective (partially bonded) specimen, it was 0.0236. The 7-fold damping increase, despite the reduced adhesive area in the defective

case, arises from enhanced energy dissipation mechanisms including friction, looseness, stress concentrations, peel stress-induced hysteresis at void edges, and local contact nonlinearities [21].

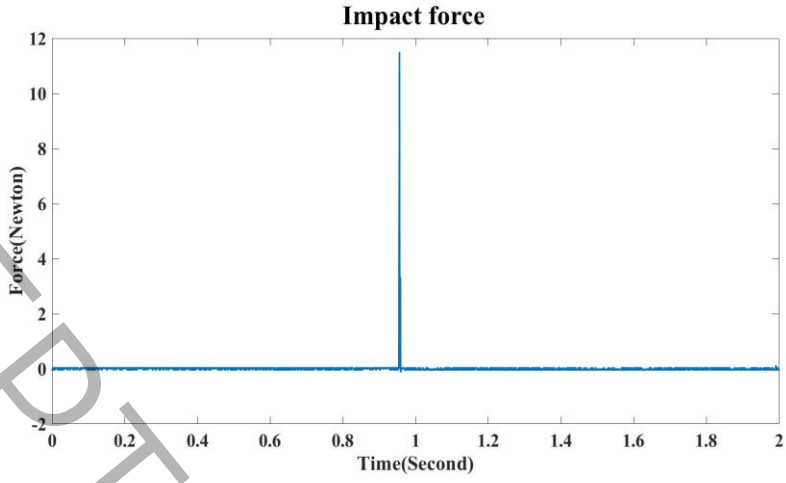

Fig. 7. The impact force diagram extracted by coding in Matlab.

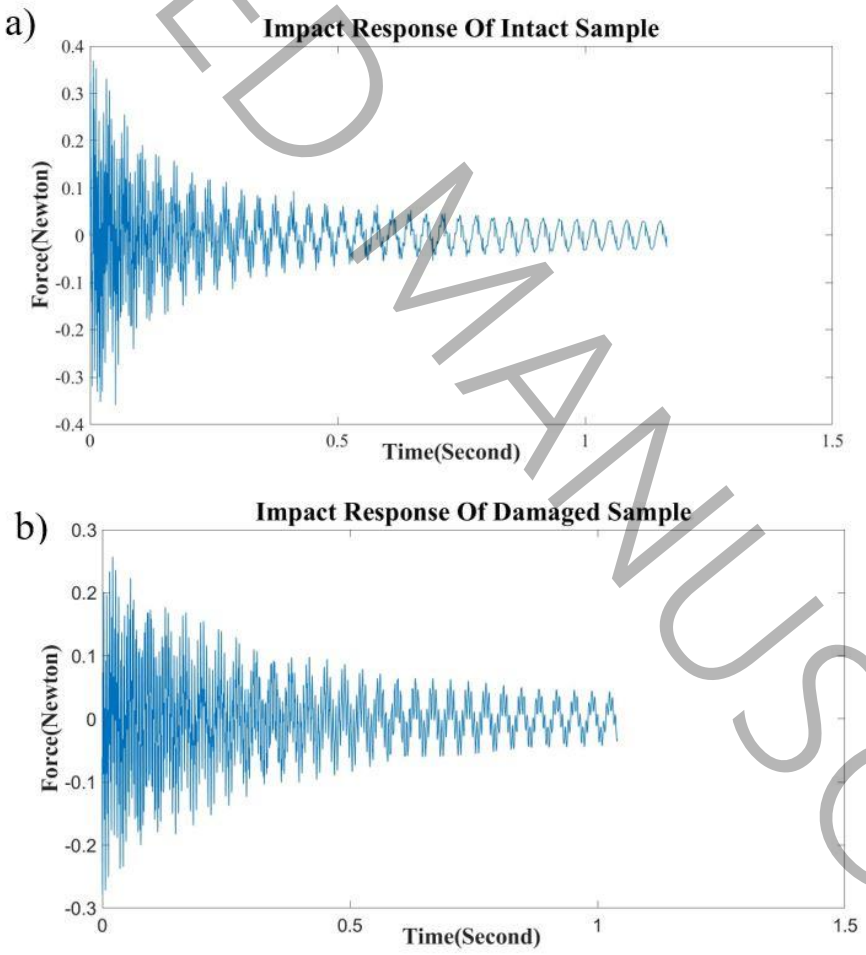

Fig. 8. The impact response diagram extracted by coding in Matlab; a) for intact specimen and b) for defective specimen.

Fig. 9 and 10 present the Frequency Response Function (FRF) curves. In Fig. 9, curves in different colors represent the vibrational responses recorded from four distinct points on the intact specimen: one before the adhesive region, one on the adhesive region, and two after it. As observed in Fig. 9, the natural frequencies

extracted from different measurement points show good repeatability, although the response amplitudes vary across locations. Fig. 10 compares the FRF curves of the fully bonded (intact) and partially bonded (defective) specimens, recorded at the first measurement point. The peaks in these curves correspond to the system's natural frequencies. A notable shift toward lower frequencies is observed in the defective specimen, indicating a reduction in natural frequencies due to the presence of the defect.

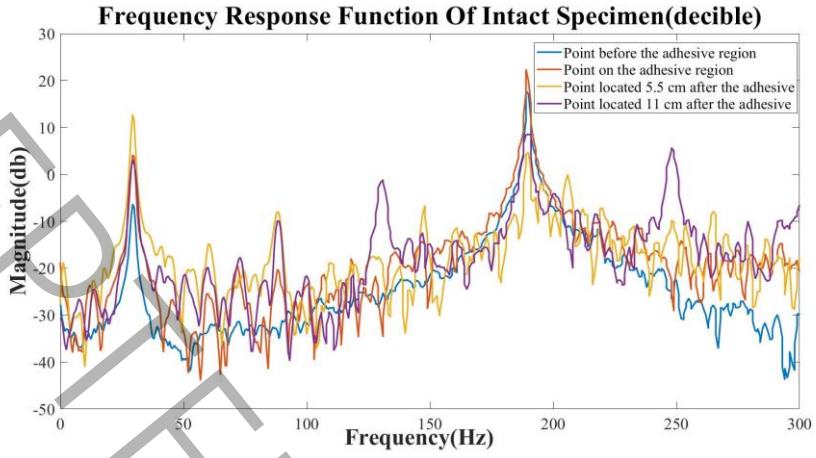

Fig.9. A sample frequency response function (FRF) plot in MATLAB for the Intact specimen, measured at four different response acquisition points. The blue curve represents the point before the adhesive region, the red curve corresponds to the point on the adhesive, and the orange and purple curves represent two points located 5.5 cm and 11 cm after the adhesive region, respectively.

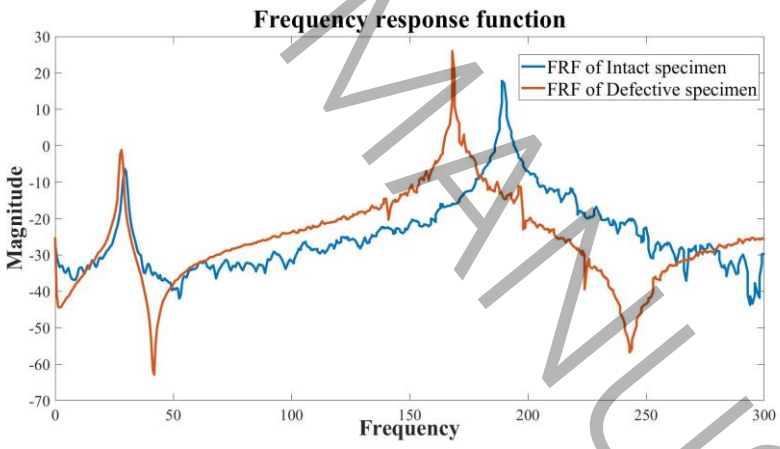

Fig.10. A comparative frequency response function (FRF) plot generated in MATLAB for the Intact and defective (partially bonded) specimens at one of the response measurement points. The blue curve represents the Intact specimen, while the red curve corresponds to the defective one.

3.2. Results of Modal Analysis and The Comparison of Natural Frequencies

After verifying the test conditions and confirming the quality of the recorded data, the natural frequencies of the specimens were obtained through appropriate analyses. As previously discussed, the extraction of these frequencies was conducted using three distinct methods:

1. Analysis of the Fast Fourier Transform (FFT) plots derived from impact response signals in the experimental modal analysis, processed in MATLAB;
2. Evaluation of impact response signals in MEscope software, employing suitable signal processing techniques for identifying natural frequencies;

3. Prediction of natural frequencies using well-defined numerical simulations, based on finite element modeling in Abaqus/CAE, through numerical modal analysis.

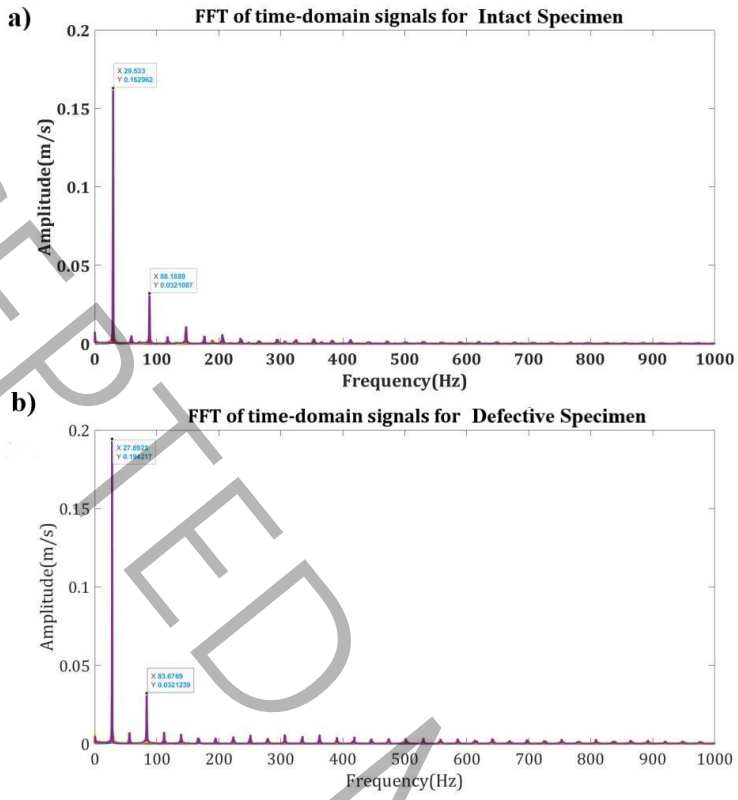

Fig.11. Fast Fourier Transform (FFT) curves for all response measurement points in : a) Intact Specimen and b) Defective Specimen

Therefore, in the first method for extracting the natural frequencies of the specimens, the Fast Fourier Transform (FFT) is applied to the velocity signals recorded at points exhibiting the highest coherence and lowest noise. Sample FFT curves are shown in Fig. 11. Numerical values of the natural frequencies are extracted and recorded using graphical tools within the MATLAB environment, such as the mouse cursor and coordinate display of peak points. For example, the coordinates of two peak points within the blue box in Fig. 11 for the intact specimen correspond to the first and second natural frequencies of 29.5 Hz and 88.18 Hz, respectively. Corresponding peaks for the defective specimen yield frequencies of 27.8 Hz and 83.6 Hz. Other natural frequency values are similarly extracted for both the intact and defective specimens.

Similarly, the natural frequencies obtained from the experimental modal analysis and processed using MEscope software, as well as the predicted frequencies from numerical modal analysis via modeling in Abaqus/CAE before and after experimental calibration, are presented for both intact and defective specimens. Table 3 summarizes all the natural frequencies derived from the aforementioned methods for both specimen conditions.

In the first two columns of Table 3, the natural frequencies obtained from experimental modal testing and MATLAB-based signal processing are presented for both the intact and defective specimens. The presence of the defect results in a reduction of all natural frequencies, with a more pronounced decrease observed at higher frequency orders. The results from the experimental modal analysis processed using MEscope software, shown in the next two columns of Table 3, are consistent with those obtained from MATLAB data processing. The natural frequencies extracted by both methods exhibit good agreement. Similarly to the previous data, the defective specimen shows lower frequency values than the intact one across all frequency orders.

Table 3. Comparison Of Natural Frequencies Obtained Through Three Different Modal Analysis Methods. (Hz)

Natural Frequency No.	Analyzing Experimental Modal Testing Data via Matlab		Analyzing Experimental Modal Testing Data via MEscope		Numerical Modal Analysis via Abaqus/CAE	
	Intact	Defective	Intact	Defective	Intact*	Defective*
F1	٢٩,٥	٢٧,٨	29.5	٢٨,١	(٢٧,٦)٢٧,٦٥٤	(٢٥,١١٣)٢٦,٢٦
F2	٨٨	٨٣,٦	88	٨٤,٣	(٨١,٠٦)٨١,١٠٨	(٧٠,١١٣)٧٦,٣٠
F3	١٨٨	١٦٦,٦	190	١٦٩	(١٥١,٧٦)١٥١,٨٦	(١٤٤,٣٨)١٥٠,٢٦
F4	٢٣٤	٢٢٣	247	٢٢٤	(٢٨٧,١٠)٢٨٧,٤١	(٢٢٣,١٧)٢٤١,٩٤
F5	٣٥٣	٣٣٤,٩	354	٣٣٧	(٣٧٦,٤٨)٣٧٦,٩٢	(٣٥٢,٧٢)٣٦٤,٥٤
F6	٥٣٠	٥٠١,٧٨	519	٥٠٢	(٥٩٢)٥٩٣,٠٤	(٤٦٨,٤٠)٥٢٠,٨٩
F7	٩١٥	٨٩٢	908	٨٩٣	(٩٦٨,٧٩)٩٧٠,٤٢	(٨٢٠,٣٤)٩٢١,٧٢
F8	١١٧٧	١٠٠٣,٨٥	1210	١٠٠٨	(١٣٧٩,٣)١٣٨١,٣	(٩٥٤,٣٠)٩٦٥,٢٤

* The values before and after experimental calibration are indicated inside and outside the parentheses, respectively.

The differences between the natural frequencies extracted via MATLAB and MEscope are mainly attributed to the distinct signal processing techniques employed [13, 30]. In MATLAB, natural frequencies are derived through the fast Fourier transform (FFT) applied directly on the raw data, whereas MEscope uses frequency response functions and advanced algorithms such as curve fitting to extract frequencies more precisely. Additionally, MEscope incorporates internal filtering, providing greater robustness against noise. Despite these methodological differences, the overall consistency of the results is acceptable.

The last two columns in Table 3 present the natural frequencies extracted from numerical modal analysis performed in Abaqus/CAE for both intact and defective specimens, before and after experimental calibration. Comparing these values reveals that the calibrated numerical model achieves better agreement with the experimental data, particularly in the lower modes. However, higher modes exhibit greater relative deviations from the experimental results, likely due to their increased sensitivity to local factors such as adhesive heterogeneity, partial adhesion, or the simplified modeling of adhesive properties in the finite element software.

These findings confirm that numerical modal analysis can predict the dynamic behavior of the system with acceptable accuracy, even in the presence of defects. The physical basis for these observations lies in the half-overlap void, which introduces a 50% unbonded area within the fixed overlap length, effectively halving the bonded contact and reducing the effective bonded length. This leads to a substantial decrease in axial stiffness (EA) and bending stiffness (EI), with the stiffness loss and mass change as (Δk) >> (Δm) dominating the dynamic response. Consequently, natural frequencies decrease systematically by 3-15% per $\omega_n=\sqrt{(k/m)}$, with the effect amplified in higher modes due to localized peel and shear stresses at the void boundaries, which distort mode shapes and exacerbate global instability [13, 26].

Overall, Table 3 and Fig.s 10-11 demonstrate systematic 3-15% frequency reductions in half-bonded specimens, validated by dual experimental-numerical agreement and cross-verified via independent MATLAB signal processing and MEscope analysis. Unlike prior studies with limited experimental validation [2, 5], this approach establishes reliable NDT thresholds for manufacturing defects absent in crack/notch literature [8, 16, 32].

Table 4 provides a rigorous error analysis, quantifying key discrepancies in the modal identification process. The consistently low errors between MATLAB and MEscope ($\varepsilon < 2.7\%$) confirm excellent signal processing consistency in both methods. The marginal but systematic pre-/post-experimental calibration errors highlight the model's robust simulation in numerical method. Crucially, the experimental-numerical correlation errors remain within typical validation thresholds (<11% across all modes). This structured analysis directly substantiates the fidelity of the numerical model and the reliability of the experimental methodology for defect detection.

Table 4. Quantitative Error Analysis: Methodological Consistency, Experimental Calibration Efficacy, and Experimental-Numerical Validation

	Intact Specimen			Defective Specimen		
Mode number	ε MATLAB & MEscope (%)	ε pre & after Calibration (%)	ε Numerical & Experimental (%)	ε MATLAB & MEscope (%)	ε pre & after Calibration (%)	ε Numerical & Experimental (%)
F1	0.0	٠,٢	٦,٣	1.1	٤,٥	6.5
F2	0.0	٠,١	٧,٨	0.8	٨,٥	9.5
F3	1.1	٠,١	٢٠,١	1.4	٤	11.1
F4	5.3	٠,١	١٦,٤	0.4	٨,١	8
F5	0.3	٠,١	٦,٥	0.6	٣,٣	8.2
F6	2.1	٠,٢	١٤,٣	0.0	١٠,٦	3.8
F7	0.8	٠,٢	٦,٩	0.1	1١.6	3.2
F8	2.7	٠,١	١٤,٢	0.4	1.1	4.2
Average	1.5375	٠,١٣٧٥	١١,٥٦٢٥	0.6000	6.4625	6.8125

3.3. Resulted Mode Shapes

features of a system's dynamic behavior, representing the deformation pattern of a structure at its natural frequencies [13]. To provide a better understanding of how the structure vibrates at its natural frequencies—and for informational purposes only—several mode shapes of the Intact specimen obtained through numerical modal analysis using Abaqus/CAE are illustrated in Fig. 12.

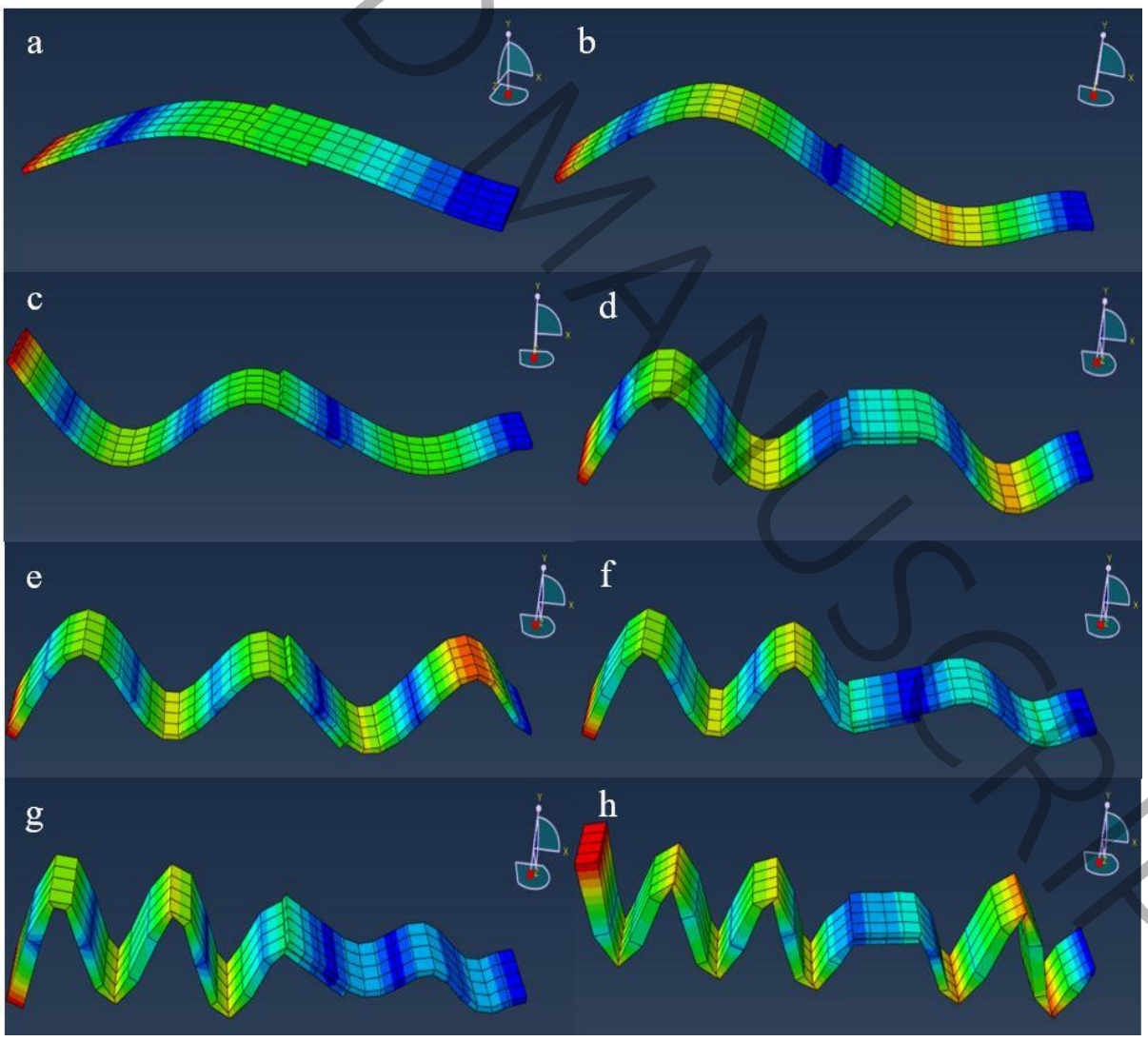

Fig. 12. Mode Shapes Resulted via Abaqus/CAE; subfigures (a) to (h) show the first to eighth mode shapes in order.

4. Conclusion

In this study, the effect of an adhesive defect—specifically, a volumetric adhesive void occupying 50% of the overlap region in single-lap joints —on the dynamic behavior of the structure was investigated through both experimental and numerical modal analysis. The results demonstrated systematic frequency reductions of 3–15% in defective specimens compared to intact ones across all modes in both approaches. This decrease is primarily attributed to the dominant effect of reduced global stiffness over the minor mass reduction in the defective region and becomes more pronounced in higher modes. The coherence diagrams of the signals, with curves closely approaching unity throughout most of the testing duration, indicate a strong correlation between input and output, reflecting high data quality and low noise levels. Additionally, the similarity in the impact force and its response across specimen's testing conditions confirms consistent and satisfactory repeatability. Notably, the damping ratio increased by approximately 7-fold (from 0.0032 to 0.0236) in the defective sample, which may be attributed to additional energy dissipation mechanisms such as friction, looseness, stress concentration, and imperfect contact. The relative agreement between the numerical and experimental results in most modes (e.g., less than 11% error in all modes) confirms the validity of the finite element modeling conducted in Abaqus/CAE. Observed discrepancies in certain modes can be attributed to differences in boundary conditions, mesh configuration, adhesive modeling, and particularly the stiffness matrix formulation in the software. Overall, the findings indicate that incomplete adhesive application in the overlap region can be effectively identified using modal analysis. This method holds promise as a diagnostic tool for structural health monitoring of bonded joints in engineering applications. Future work could investigate a broader range of macroscopic defect scenarios—including variations in defect shapes, sizes, and locations within the overlap region—to better elucidate their effects on the modal response of adhesive joints. Additionally, extending this study to other joint configurations (e.g., double-lap and stepped joints) and alternative modal testing approaches (such as MIMO setups) would help assess the generality of the observed trends.

5. Refrences

[1] Y. Wei, X. Jin, Q. Luo, Q. Li, G. Sun, Adhesively bonded joints–a review on design, manufacturing, experiments, modeling and challenges, Composites Part B: Engineering, 276 (2024) 111225.

[2] L. Ramalho, I.J. Sánchez-Arce, D.C. Gonçalves, J. Belinha, R. Campilho, Numerical analysis of the dynamic behaviour of adhesive joints: A review, International Journal of Adhesion and Adhesives, 118 (2022) 103219.

[3] M. Damghani, M.S. Khan, G.A. Atkinson, Experimental study of bonded, bolted, and hybrid bonded-bolted single lap shear joints with woven CFRP adherends, Composite Structures, 334 (2024) 117989.

[4] F. Marchione, Investigation of vibration modes of double-lap adhesive joints: effect of slot, International Journal of Engineering, 33(10) (2020) 1917–1923.

[5] A.B.A. Basri, D.W. Chae, H. Lee, Investigation of the dynamic characteristics of a carbon-fiber-reinforced epoxy with adhesive-jointed structure, Composite Structures, 247 (2020) 112499.

[6] R.B. Randall, V.-b.C. Monitoring, Industrial, aerospace and automotive applications, VIBRATION-BASED CONDITON MONITORING. West Sussex, (2011) 13–20.

[7] R.D. Adams, J. Comyn, W.C. Wake, Structural adhesive joints in engineering, Springer Science & Business Media, 1997.

[8] M.T. Das, A. Yılmaz, Experimental modal analysis of curved composite beam with transverse open crack, Journal of Sound and Vibration, 436 (2018) 155–164.

[9] D. Agarwalla, D. Parhi, Effect of crack on modal parameters of a cantilever beam subjected to vibration, Procedia Engineering, 51 (2013) 665–669.

[10] M. Aslam, P. Nagarajan, M. Remanan, Dynamic response of piezoelectric smart beam with adhesive debonding, Material Design & Processing Communications, 2(4) (2020) e159.

[11] Y. Patil, R. Barjibhe, Modal analysis of adhesively bonded joints of different materials, Int J Mod Eng Res, 3(2) (2013) 633–636.

[12] A.S.f. Testing, Materials, Standard test method for measuring vibration-damping properties of materials, ASTM International, 2010.

[13] D.J. Ewins, Modal testing: theory, practice and application, John Wiley & Sons, 2009.

[14] J. Lee, Free vibration analysis of delaminated composite beams, Computers & Structures, 74(2) (2000) 121–129.
[15] S. Wang, Y. Li, Z. Xie, Free vibration analysis of adhesively bonded lap joints through layerwise finite element, Composite Structures, 223 (2019) 110943.
[16] S.S.B. Chinka, S.R. Putti, B.K. Adavi, Modal testing and evaluation of cracks on cantilever beam using mode shape curvatures and natural frequencies, in: Structures, Elsevier, 2021, pp. 1386–1397.
[17] O. Sahu, P. Das, S. Choudhury, N. Pradhan, B. Basa, B. Jena, On transverse crack effects in beams under free vibration using finite element analysis, Materials Today: Proceedings, (2024).
[18] R.K. Behera, S. Parida, R. Das, Effect of pre-embedded adhesion failures and surface ply delaminations on the structural integrity of adhesively bonded single lap joints made with curved laminated FRP composite panels, International Journal of Adhesion and Adhesives, 108 (2021) 102887.
[19] K. Pazand, A.S. Nobari, Investigation of damage effect on the effective dynamic mechanical properties of an adhesive in linear and nonlinear response regimes, Journal of Vibration and Control, 23(14) (2017) 2209–2220.
[20] B. Ordonneau, E. Paroissien, M. Salaün, A. Benitez-Martin, S. Schwartz, J. Malrieu, A. Guigue, A simplified modal analysis of a single lap bonded joint using the macro-element technique, International Journal of Solids and Structures, 249 (2022) 111631.
[21] E. Nwankwo, A.S. Fallah, L. Louca, An investigation of interfacial stresses in adhesively-bonded single lap joints subject to transverse pulse loading, Journal of Sound and Vibration, 332(7) (2013) 1843–1858.
[22] A. Melro, K. Liu, Determination of the modal parameters of a single lap adhesively bonded joint using the transfer matrix method plus model updating, International Journal of Adhesion and Adhesives, 101 (2020) 102628.
[23] J. García-Barruetabeña, F. Cortés, Finite elements analysis of the vibrational response of an adhesively bonded beam, Engineering Structures, 171 (2018) 94–104.
[24] R. Gunes, M.K. Apalak, M. Yildirim, I. Ozkes, Free vibration analysis of adhesively bonded single lap joints with wide and narrow functionally graded plates, Composite Structures, 92(1) (2010) 1–17.
[25] A.F.G. Tenreiro, A.M. Lopes, L.F. da Silva, R.J. Carbas, Influence of void damage on the electromechanical impedance spectra of Single Lap Joints, NDT & E International, 138 (2023) 102865.
[26] R. Brincker, C. Ventura, Introduction to operational modal analysis, John Wiley & Sons, 2015.
[27] X. He, Finite element analysis of torsional free vibration of adhesively bonded single-lap joints, International journal of adhesion and adhesives, 48 (2014) 59–66.
[28] K.N.K.A.K.R.U.A. Vasudevan, Temperature-Frequency–Dependent Viscoelastic Properties of Neat Epoxy and Fiber Reinforced Polymer Composites: Experimental Characterization and Theoretical Predictions, polymers, (adhesives) (2020) 31.
[29] B. Boashash, Time-frequency signal analysis and processing: a comprehensive reference, Academic press, 2015.
[30] L. Cohen, Time-Frequency Analysis: What We, Landscapes of Time-Frequency Analysis: ATFA 2019, (2020) 75.
[31] S.S. Rao, F.F. Yap, Mechanical vibrations, Addison-Wesley New York, 1995.
[32] M. Gul, F.N. Catbas, Structural health monitoring and damage assessment using a novel time series analysis methodology with sensor clustering, Journal of Sound and Vibration, 330(6) (2011) 1196–1210.